Springer

Journal of
Mechanical
Science and
Technology

Journal of Mechanical Science and Technology 23 (2009) 1924~1931

www.springerlink.com/content/1738-494x
DOI 10.1007/s12206-009-0503-4

Characteristics of complicated AISI316L automobile components manufactured by powder/metallurgy †

L. Zhong Liang[1], L. Jin Hui[2], S. Yu Sheng[3,*] and Y. Chun Ze[3]

[1]*State Key Laboratory for Manufacturing Systems Engineering, XI'an JiaoTong University, XI'an, 710049, China*
[2]*Heilongjiang University of Science and Technology, Harbin, 150027, China*
[3]*School of Material Science and Technology, HUST, Wuhan, 430074, China*

(Manuscript Received December 3, 2008; Revised April 12, 2009; Accepted April 20, 2009)

Abstract

Indirect Selective Laser Sintering/ Isostatic Pressing (SLS/IP), with Cold Isostatic Pressing (CIPing) and Hot Isostatic Pressing (HIPing) IPs, is adopted for the manufacture of complicated automobile components. The preparation of PA12-coated AISI316L powder and airproof plastic canning during CIPing are also investigated. The influence of technology parameters on the performances of AISI316L specimens during SLS/IP is likewise analyzed. Results show that PA12-coated AISI316L powders are successfully prepared through the dissolution and precipitation process, and that it is better to fabricate airproof canning for complicated components with natural latex. After sintering AISI316L specimens from 1300℃ to 1340℃ (CIPed at more than 300 MPa ahead), their relative densities increased, approaching 92%. Subsequently, their relative densities are improved by HIPing, whose optimal pressure and temperature parameters are between 90 MPa and 20 MPa, and 1150℃ and 1250℃, respectively. The optimal tensile performances are close to those of annealed AISI316L compact materials.

Keywords: Automobile components; Powder metallurgy; AISI316L stainless steel; Tensile performance

1. Introduction

Metal components manufactured by Powder/Metallurgy (P/M) are generally used in the automobile industry; of these, austenite stainless steel has the advantages of good mechanical performance and resistance to corrosion, among others [1]. For this reason, the manufacture of automobile components made of austenite stainless steel using advanced P/M technologies has become a significant endeavor.

Adopted moulds used when automobile components were still manufactured by conventional P/M technologies were expensive [2, 3]. This led to high production costs. At the same time, using these moulds made it impossible to produce several complicated components. Thus, adopting advanced manufacturing technologies for the development of automobile components and the evaluation of new automobile products has become an important consideration. Lately, several advanced P/M technologies have been presented, such as Selective Laser Melting [4-9], which does not require moulds and facilitates the manufacture of complicated components. However, the balling phenomenon occurred when molten powders solidified; at the same time, residual stress in metal components was found to be too large [7, 8]. Therefore, it was difficult to achieve high precision and good performance. In addition, although indirect SLS has been considered a suitable, high-precision method in manufacturing complicated metal components [9], their relative densities were often lower. Thus, SLS components were often infiltrated by low-melting metal for improving their relative densities [10]. This process easily worsened the tensile per-

† This paper was presented at the 9th Asian International Conference on Fluid Machinery (AICFM9), Jeju, Korea, October 16-19, 2007.recommended for publication in revised form by Associate Editor Dae-Eim Kim

*Corresponding author. Tel.: +82 32 872 309686 27 87557042, Fax.: +82 32 868 171686 2787558581

formance of such components due to the formed eutectic. As a solution to these problems, the SLS/Hot Isostatic Pressing (HIPing) method has been adopted [11, 12]. However, one other problem that required consideration was the oxidation of titanium alloy during the canning process. Enlightened by SLS/HIPing, Cold Isostatic Pressing (CIPing) is thus introduced into SLS/HIPing (which is abbreviated to SLS/IP in this paper) for manufacturing complicated automobile components.

2. Experimentations

2.1 Materials

Table 1 shows the properties and contents of SLS raw materials for preparing PA12-coated AISI316L, in which AISI316L and PA12 were uses as construction material and binder, respectively. Table 2 shows the compositions of AISI316L [3]. Natural latex (NL), S, antioxidant 264, accelerator PX, and active agent ZnO were chosen for manufacturing airproof canning used in the CIPing stage.

2.2 Experimental procedures

2.2.1 Preparation of PA12-coated AISI316L powders

Some high-polymer coated metal powders were investigated in the past; of these, PMMA, PA11, and epoxy-acrylate were often adopted [13]. However, production cost was very high. Then PA12 was chosen to coat metal powders by benzene solvent [14], but this brought about pollution and gave rise to environmental concerns. Finally, alcohol was used as the solvent of PA12 for coating AISI316L powders through a dissolution and precipitation process [15]. The proposed procedure was as follows:

(1) AISI316L and PA12 powders, mixed solvents, and an antioxidant were added into a reactor. Subsequently the reactor was vacuumed, and then N_2 gas was used to protect the reactants from oxidation. The mixed solvents included ethanol, glycol, methyl glycol, and distilled water. The ratio of AISI316L and PA12 was 100:(1-3), and that of PA12, mixed solvents, and antioxidant was 100: (500-800): (0.1-0.5) according to their weights.

(2) The abovementioned solution was heated between 150 and 160℃ at the rate of 1-2℃/min in order to completely dissolve the PA12. Afterwards, the solution was allowed to cool for 2-3h.

(3) The mixed solution was stirred synchronously when it cooled at the rate of 2-4℃/min. During this time, PA12 continued to precipitate on the surface of the AISI316L particles, after which suspended liquid was formed. This suspended liquid was distilled out in order to separate the PA12-coated AISI316L particles and the solvent. The particles were then dried, milled, and sieved. Finally, PA12-coated AISI316L powders were successfully prepared as shown in Fig. 1a. Meanwhile, Fig. 1b shows the homogenous distribution of PA12 on the surface of AISI316L powders.

2.2.2 SLS specimen preparation stage

First, green components used as testing specimens (130 mm × 30 mm × 20 mm), were formed by indirect SLS aside from some impellers. Technology parameters in indirect SLS stage mainly included preheating temperature (150℃-165℃), laser power (15W-17W), scan velocity (1800 mm/s-2000 mm/s), scan interval (0.1 mm-0.15 mm), and layer thickness (0.1 mm-0.15 mm).

Some impellers were manufactured by indirect SLS with PA12-coated AISI316L powders, as shown in Fig. 2. Their strength was so high that it was difficult to destroy them in the process of SLS/IP.

Degreasing was then carried out in the H_2 furnace so that the PA12 binder could be removed completely from the SLS green specimens.

Table 1. Properties and contents of SLS raw materials for preparing PA12-coated AISI316L.

Compositions	Size/ μm	Shape	Melting point	Density	Wt%
AISI316L	≦45 μm	Irregular	1375℃	7.99g/cm^3	98.5-99.2%
PA12	≦30 μm	Irregular	178℃	1.02 g/cm^3	0.8-1.5%

Table 2. Compositions of AISI316L.

Compositions	C	Si	Mn	P	S	Ni	Cr	Mo	N	Fe
Wt%	0.018	0.71	1.46	0.03	0.025	10.18	16.81	2.1	0.085	The balance

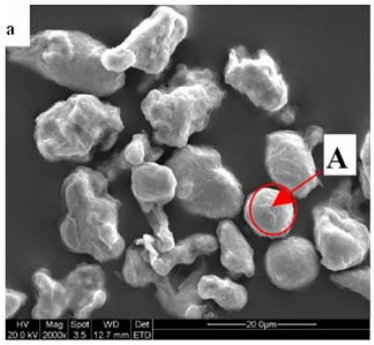

(a) PA12-coated AISI316L powders

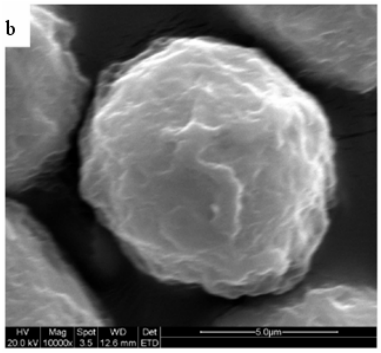

(b) Partial magnification of region A

Fig. 1. Micrographs of PA12-coated AISI316L powders.

Fig. 2. An SLS impeller of AISI316L.

2.2.3 Canning stage

Given that RTV-2 viscosity is large and the reaction time of its cross bonding is slow, it is therefore difficult to spread on the surface of complicated components during the manufacture of airproof canning. On the contrary, viscosity of NL is lower, and the reaction of its cross bonding is quick. As such, it can easily spread on the surface of complicated components. In addition, polymerized NL has good elasticity, as well as soft and anti-tearing characteristics, so the working pressure from liquid is not lowered during CIPing. For these reasons, NL was chosen as a raw material.

Fig. 3. Fabrication of airproof canning.

First, the S element was chosen as a vulcanizing agent when manufacturing airproof canning for complicated components by NL. Second, antioxidant 264 and active agent ZnO were used to improve the components' performances, because NL easily suffered from aging. In addition, toward a more rapid sulfuration reaction of NL, accelerator PX was also adopted. The rate of NL, S, antioxidant 264, accelerator PX, and active agent ZnO was 100:(1-1.2):(0.65-1):1:(0.5-1.5). The steps required to manufacture airproof canning are described below.

(1) S was first added into NL, followed by the accelerator PX, the active agent ZnO, and the antioxidant 264, in this order. Subsequently, the mixed liquid was heated between 60℃ and 70℃ for prevulcanization of NL, which facilitated the rapid formation of airproof canning throughout the rest of the process.

(2) The AISI316L specimens were dipped into a solution consisting of $CaCl_2$ and distilled water, which was used as an agglomerating agent. The specimens were then immersed into the above-mentioned prevulcanized NL. Subsequently, the Ca^+ of $CaCl_2$ condensed the electric double layers and reduced electrical potential difference resulting from the negative charge adsorbing on the surface of NL particles. Finally, airproof plastic canning of NL was formed.

(3) The encapsulated specimens were placed into a drying baker between 70℃ and 100℃. Through this process, the polyreaction rate of NL became quicker and NL polymerized much faster. After repetitions of steps 1-3, airproof plastic canning was formed as shown in Fig. 3.

2.2.4 CIPing stage

The encapsulated SLS specimens were CIPed at different pressures (300 MPa, 400 MPa, and 500 MPa) in order to improve their relative densities.

2.2.5 Sintering and HIPing stages

The AISI316L specimens were sintered at different temperatures (1300℃, 1320℃, and 1340℃) for 2 hours or so. The vacuum inside the sintering furnace was 10^{-3} Pa or so. Afterwards, using the ABBQIH-6 equipment, the AISI316L specimens were respectively HIPed at 1150℃/90 MPa, 1150℃/120 MPa, 1250℃/90 MPa or 1250℃/120 MPa for 1 hour in order to improve their performances.

2.2.6 Measurements

In accordance with the Archimedes law, relative densities of the AISI316L specimens before and after HIPing, were respectively calculated according to Eq. (1). Although there were five tensile tests using the same conditions, the mean relative density can be achieved using the following equation:

$$\rho_r = m_1 \bullet \rho_0 \bullet \rho_1 /(m_2 - m_3), \quad (1)$$

where ρ_r refers to the relative densities of AISI316L specimens manufactured by SLS/IP; ρ_0 and ρ_1 refer to the densities of water at room temperature and AISI316L compact material; m_1 refers to their weights before the AISI316L specimens were infiltrated into ceresin wax; and m_2 and m_3 refer to their weights in air and in water after AISI316L specimens were infiltrated into the ceresin wax.

Using the same variable conditions for calculating the mean of tensile performances, 5 tensile samples (ASTM E8) were prepared through the linear cutting of HIPed specimens. Afterwards, their tensile performances were tested on a Z010 universal testing machine at the loading rate of 2 mm/min. Their microstructures were then observed using a Quanta 200 environmental scanning electron microscope.

3. Results and discussions

3.1 Relative densities of the AISI316L specimens in the sintering stage of SLS/IP

Fig. 4 shows the relative densities of AISI316L specimens CIPed at 300 MPa, 400 MPa, and 500 MPa when sintered at 1300℃, 1320℃ and 1340℃, respectively, which gradually increased and approached

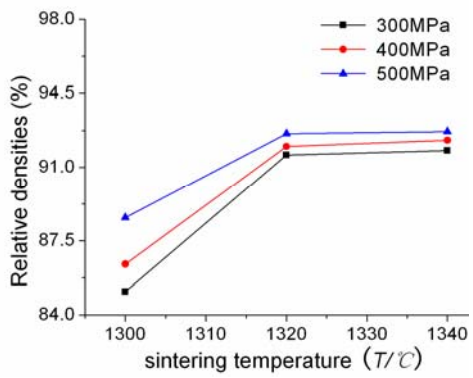

Fig. 4. Relative densities of the AISI316L specimens CIPed at different pressures during sintering.

about 92%. Fig. 5(a), Fig. 5(b) and Fig. 5(c) represene t thCIPed, sintered, and HIPed AISI316L impellers, respectively.

When CIPing pressure increased from 300 MPa to 500 MPa, on the one hand, an increasing number of particles underwent plastic yield or strain-hardening, which caused more defects in crystal grains with larger distortion of lattice. On the other hand, residual stress among the AISI316L specimens became larger, thereby causing an increase in chemical potential difference as shown in Eq. (2) below.

$$\Delta\mu = \sigma V_m \quad (2)$$

In the above, $\Delta\mu$, σ, and V_m refer to chemical potential difference, residual stress and mole volume of specimens, respectively [16].

In the stage of sintering, the abovementioned factors facilitate the rapid occurrence of atom diffusion and the densification of metal specimens, thereby causing a gradual increase in their relative densities. However, it is possible that initial relative densities of AISI316L specimens would increase less when these are CIPed from 300 MPa to 500 MPa, during which their pores can easily be filled by atom diffusion during subsequent sintering. Thus, their relative densities during sintering vary less according to Eq. (3) (as shown in Fig. 4).

$$v_s \big/ v_p = v \quad (3)$$

As shown above, v_p and v_s represent pore volume of specimens before and after sintering; where v is a constant [16].

(a) CIPed

(b) Sintered

(c) HIPed

Fig. 5. CIPed, sintered, and HIPed impellers of AISI316L.

When sintering temperature is at 1300℃, liquid sintering does not appear for AISI316L specimens. In contrast, when sintering temperature increases between 1320℃ and 1340℃, which is less than the melting point of AISI316L, supersolidus sintering begins to form. The coefficient of atom diffusion increased along with an increase in sintering temperature (Eq. (4)). This is considered advantageous to the densification of the AISI316L specimens. Thus, their relative densities increased remarkably during sintering between 1300℃ and 1320℃, but their relative densities approached the same value between 1320℃ and 1340℃. Finally, it is concluded that the optimal sintering temperature should be between 1320℃ and 1340℃.

Fig. 5(a) shows the AISI316L specimens CIPed at 300 MPa, while Fig. 5(b) shows the corresponding specimens sintered at 1320℃, during which they have shrinked remarkably.

$$D = D_0 \exp(-\Delta G / RT) \tag{4}$$

In the equation above, D refers to the self-diffusion coefficient, D_0 is a constant, ΔG refers to the activation energy of self-diffusion, and R and T refer to gas constant and thermodynamics temperature, respectively [16].

3.2 Relative densities of the AISI316L specimens in the HIPing stage of SLS/IP

Fig. 6 shows micrographs of the AISI316L specimens during HIPing at different temperatures and pressures. As can be seen, the sizes and distributions of pores and crystal grains are different. Table 3 shows the influence of HIPing temperatures and pressures on the relative densities of AISI316L specimens that have been previously CIPed at 300 MPa and sintered at 1320℃. In the table, Ⅰ/2 and Ⅱ/2 represent the mean of their relative densities under the condition of different HIPing parameters, and the range represents the influence of HIPing parameters on their relative densities. As can be seen, when HIPing temperatures and pressures increase from 1150℃ to 1250℃ and from 90 MPa to 120 MPa, respectively, their final relative densities exceeded 95% and increased gradually. The range of relative densities thus became 1.55% and 0.4% for each sample group.

When HIPing pressures increased and then exceed those in closed pores, plastic yield began to take place with creep deformation appearing in the AISI316L specimens. The closed pores reduced or shrinked, as can be concluded from Fig. 6(a) versus Fig. 6(b) (or Fig. 6(c) versus Fig. 6(d)). Their relative densities also increased. When HIPing temperatures increased, yield strength of the AISI316L material became remarkably reduced. Thus, more AISI316L particles were produced from the plastic yield, and more pores

Table 3. Influence of HIPing parameters on relative densities of the AISI316L specimens.

No.	HIP temperatures	HIP pressures	Relative density
1	1150℃	90MPa	95.3%
2	1150℃	120MPa	95.6%
3	1250℃	90MPa	96.7%
4	1250℃	120MPa	97.2%
Ⅰ/2	95.45% (1150℃)	96.0% (90MPa)	
Ⅱ/2	96.95% (1250℃)	96.4% (120MPa)	
Range (|Ⅱ/2-Ⅰ/2|)	1.5%	0.4%	

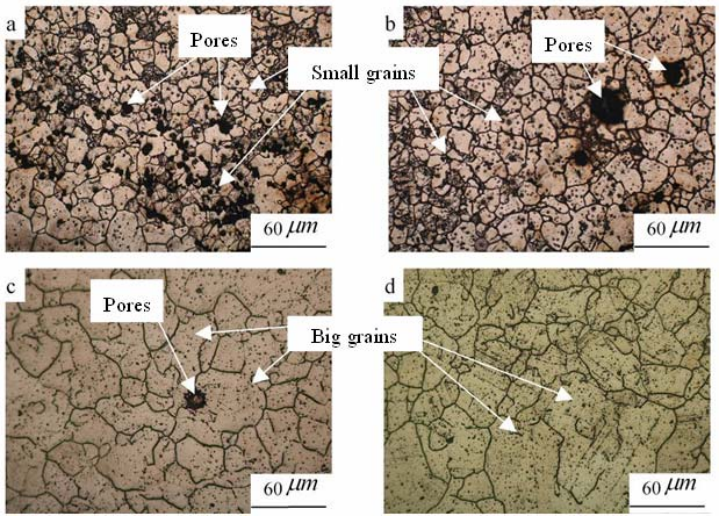

(a) 1150℃/90 MPa (b) 1150℃/120 MPa (c) 1250℃/90 MPa (d) 1250℃/120 MPa

Fig. 6. Micrographs of AISI316L specimens HIPed at different temperatures and pressures.

were healed. However, crystal grains were formed, as can be concluded from Fig. 6a versus Fig. 6(c) (or Fig. 6(b) versus Fig. 6(d)).

Given the above, we can say that the relative densities of the AISI316L specimens are mainly influenced by HIPing temperature instead of HIPing pressure. The optimal temperatures and pressures during HIPing were identified to be at between 1150℃ and 1250℃, and between 90 MPa and 120 MPa, respectively.

Fig. 5(c) shows the impeller manufactured by SLS/IP with the above optimal technology parameters, whose relative densities are about 95%, satisfying engineering application requirements.

3.3 Tensile performances of the AISI316L specimens in the HIPing stage of SLS/IP

Table 4 shows the influence of HIPing temperatures or pressures on the tensile performances of AISI316L specimens manufactured by SLS/IP, which are improved gradually with increasing HIPing parameters. As compared with tensile performances of annealed AISI316L compact material, except for tensile strength, their Young's modulus, yield strength, and elongation percentage are lower.

The relative densities of AISI316L specimens manufactured by SLS/IP increased, and their pores gradually became spheroidized when HIPing temperatures or pressures increased. Although crystal grains grew with the increase of their relative densities, their tensile performances became improved through their relative densities instead of size of crystal grains. As such, their tensile performances also gradually improved with the increase of the abovementioned HIPing parameters.

During HIPing, a great number of carbides appeared above the AISI316L specimens (as shown in Fig. 7(a)), so their tensile strengths became larger

Table 4. Influence of HIPing parameters on relative densities of the AISI316L specimens.

		E/GPa	Yield strength/MPa	Tensile strength/MPa	Elongation Percentage/%
SLS/IP Components of AISI316L	1150℃/90MPa	124.2	256.7	619.6	42.1
	1150℃/120MPa	125.5	258.5	622.25	43.4
	1250℃/90MPa	143.5	276	627.51	43.5
	1250℃/120MPa	142.5	277	649.49	45.7
Annealed AISI316L compact material		197	300	570	50

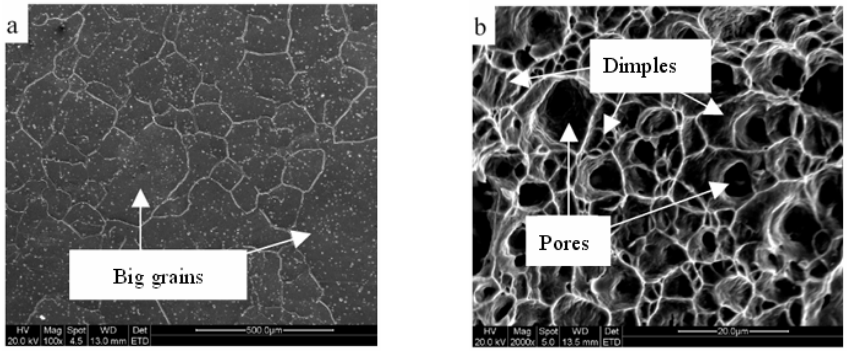

(a) Micrographs of HIPed specimens at 1250℃/120 MPa (b) Fracture patterns

Fig. 7. Micrographs and fracture patterns of the AISI316L specimens during HIPing at 1250℃/120 MPa.

than those of annealed AISI316L compact material. However, their relative densities are still lower than 100%, and there are some residual pores still existing in these (as shown in Fig. 7(b)). Thus, their Young's modulus, yield strengths, and elongation percentages became lower than those of annealed AISI316L compact material.

Consequently, dense automobile components of AISI316L with high performances can be manufactured by SLS/IP with the above optimized technology parameters.

4. Conclusions

In this study, PA12-coated AISI316L powders are successfully prepared by dissolution and precipitation of PA12 into alcohol, which is considered suitable for SLS raw material. Moreover, airproof canning of complicated components is easily manufactured with natural latex, S, antioxidant 264, accelerator PX and ZnO, all of which satisfy the CIPing requirements. Relative densities of the AISI316L specimens increased when CIPed at a larger pressure or sintered at a higher temperature. Moreover, optimal CIPing pressure and sintering temperatures are found to be at 300 MPa, and between 1320℃ and 1340℃, respectively. In the HIPing stage of SLS/IP, their relative densities are mainly influenced by HIPing temperatures instead of HIPing pressures. Their tensile performances are close to those of annealed AISI316L compact material when they are CIPed at 300 MPa, followed by sintering at 1320℃ and HIPing at 1250℃/120 MPa, which satisfies the requirements of engineering applications. Therefore, SLS/IP is a suitable solution for the rapid development of complicated automobile components.

Acknowledgment

This work was financially supported by the Fifteen National Defence Fund and and State key laboratory for powder metallurgy in Central South University.

References

[1] C. T. S. Chade, J. W. Schaberl and A. Lawley, Stainless steel AISI grades for PM applications, *International Journal of Powder Metallurgy*. 44(3) (2008) 57-67.

[2] Y. S. Kwon, H. T. Lee and K. T. Kim, Analysis for cold die compaction of stainless-steel powder, *Journal of Engineering Materials and Technology*.

119(4) (1997) 366-373.

[3] A. V. C. Sobral, M. P. Hierro, F. J. Perez, W. RistowJr and C. V. Franco, Oxidation of injection molding 316L stainless steel at high temperature, *Materials and Corrosion*. 51 (2001) 791-796.

[4] Yongzhong Zhang, Mingzhe Xi, Shiyou Gao and Likai Shi, Characterization of laser direct deposited metallic Components, *Journal of Materials Processing Technology*. 142 (2003) 582-585.

[5] N. B. Qi, Y. N. Yan, F. Lin, W. He and R. J. Zhang, Direct metal part forming of 316L stainless steel powder by electron beam selective melting, *Proceedings of the Institution of Mechanical Engineers, Part B (Journal of Engineering Manufacture)*. 220(B11) (2006) 1845-1853.

[6] M. Badrossamay and T. H. C.Childs, Further studies in selective laser melting of stainless and tool steel powders, *International Journal of Machine Tools & Manufacture*. 47 (2007) 779-784.

[7] Y. F. Shen, D. D. Gu and Y. F. Pan, Balling process in selective laser sintering 316 stainless steel powder, *Advances In Machining & Manufacturing Technology VIII*. 315-316 (2006) 357-360.

[8] P. Mercelis and J. P. Kruth, Residual stresses in selective laser sintering and selective laser melting, *Rapid Prototyping Journal*. 12(5) (2006) 254-265.

[9] G. Vaneetveld, A. M. Clarinval, T. Dormal, J. C. Noben and J. Lecomte Beckersd, Optimization of the formulation and post-treatment of stainless steel for rapid manufacturing, *Journal of Materials Processing Technology*. 196 (2008) 160-164.

[10] J. H. Liu, Y. S. Shi and K. H. Chen et al, Research on manufacturing Cu matrix Fe-Cu-Ni-C alloy composite Components by indirect selective laser sintering, *International Journal of Advanced Manufacturing Technology*. 33 (2007) 693-697.

M. K. Agarwala, D. Bourell and J. Beaman, Post-processing of selective laser sintered metal Components, *Rapid Prototyping Journal*. 1(2) (1995) 36-44.

[11] D. Suman, J. J. Beama and M. Wohlert et al, Direct laser freeform fabrication of high performance metal components, *Rapid Prototyping Journal*. 4(3) (1998) 112-117.

[12] W. Z. Wu and M. G. Yang, Development of polymer coated metallic powder for Selective Laser Sintering (SLS) process, *Journal Of Advanced Materials*. 34(2) (2002) 25-28.

[13] P. K. Bai, M. Z. Li and M. L. Fang et al, Study on Selective Laser Sintering Mechanism of Polymer-coated Stainless Steel Powder, *Journal of Materials Engineering*. 8(2005) 28-31.

[14] S. YuSheng, Y. ChunZhe, Y. JinSong and H. Shu-Huai, One preparation process of a kind of nylon coated metal powders, China. (2007) Patent No. CN200710051795.9.

[15] Guo Shiju, Theory of powder sintering. *Publishing Inc. of Metallurgy Industry,* Beijing, China, (2002) 11-19.

L. Zhong Liang received his Ph.D. degree from HUST, China, in 2008. Dr. ZhongLiang is currently a Postdoctoral student at XJTU in China, specializing in the investigation of RPM. He has achieved three patents and has published over 10 papers. Of these, five papers have been indexed in SCI.

S. Yu Sheng is currently a professor at HUST, China, and is also specializing in the investigation of RPM. He has published more than 100 papers and has achieved more then 20 patents. From his works, 30 papers have been indexed in SCI.